Strong electron-phonon-interaction modes in the *n*-type high-T_c superconductors $Nd_{2-x}Ce_xCuO_4$ and $Pr_{1-x}LaCe_xCuO_4$

S. Sugai, Y. Sone, and H. Mabuchi
Department of Physics, Faculty of Science, Nagoya University, Chikusa-ku, Nagoya 464-8602, Japan
(Received 29 November 2003; revised manuscript received 20 April 2004; published 17 September 2004)

The phonon modes with strong electron-phonon interactions were investigated by two-phonon Raman scattering in $Nd_{2-x}Ce_xCuO_4$ and $Pr_{1-x}LaCe_xCuO_4$. The modes change from the Σ_1 modes near $(0.4\pi, 0.4\pi)$ in the insulating phase to the Δ_1 modes near $(0.4\pi, 0)$ in the metallic phase. The temperature dependence of the Δ_1 modes is the same as the Raman susceptibility of electronic excitations in the quasiparticle band generated at the Fermi energy. It suggests that the change of the electron-phonon interactions is directly related to the presence of the quasi-particle band in the metallic phase.

DOI: 10.1103/PhysRevB.70.104508 PACS number(s): 74.72.Jt, 74.25.Kc, 74.25.Gz

I. INTRODUCTION

The electron-phonon interaction was reexamined to explain the kinks near 70 meV in the electronic dispersion curves in *p*-type high T_c superconductors.[1–3] In *n*-type superconductor $Nd_{2-x}Ce_xCuO_4$ (NCCO) the kink was, however, not observed along the $(0,0)$–(π,π) direction.[2] The doping induced change in the phonon dispersion curve is also very different between *p*-type and *n*-type superconductors. In *p*-type superconductor $La_{2-x}Sr_xCuO_4$ (LSCO) the Δ_1 mode at $(\pi,0)$—half-breathing mode—decreases in energy as carriers are doped.[4–8] On the other hand in *n*-type superconductor NCCO the softening is observed around $(0.4\pi,0)$.[9,10] Thus the carrier density dependence of the electronic states and phonons in *n*-type high T_c superconductors is very different from those in *p*-type high T_c superconductors. Therefore it is very interesting to investigate what phonon modes have strong electron-phonon interactions in *n*-type high T_c superconductors, how they change with the increase of carrier density, and whether the electron-phonon interaction is related to the development of the quasi-particle band and the superconductivity as temperature decreases.

In order to extract the phonon modes with strong electron-phonon interactions, we use two-phonon Raman scattering. Two-phonon Raman scattering is a useful method to find out the phonon modes with strong electron-phonon interactions in the whole Brillouin zone. The scattering intensity is proportional to the fourth power of the electron-phonon interaction. Two-phonon scattering is enhanced by the resonant Raman effect, when the incident photon energy approaches the intermediate electronic excitation energy. The present experiments were performed near the resonant condition.

In the previous paper our group disclosed that the electron-phonon interaction is strongly correlated to the superconductivity in *p*-type high T_c superconductors.[11] In *p*-type high T_c superconductors the position of the superconducting coherent (pair-breaking) peak in *k*-space changes generally from $(\pi/2,\pi/2)$ to $(\pi,0)$, as carrier density increases, in correlation with the change of the low-energy electronic density of states. However, the change of the coherent peak in *k*-space is more rapid than that of the electronic density of states, which suggests the existence of an additional pair-enhancing and pair-breaking mechanism. We found from two-phonon Raman scattering that the phonon mode with the strongest electron-phonon interaction changes from the breathing mode at (π,π) to the half-breathing mode at $(\pi,0)$ in good correlation with the change of the coherent peak. It was calculated that the off-diagonal electron-phonon interaction of the half-breathing mode—the zone-boundary LO mode at $(\pi,0)$—helps the spin-mediated superconductivity.[2,12] Thus the electron-phonon interaction plays an important role to generate the superconductivity in the limited region of *k*-space and causes the shift of the superconducting region in *k*-space.

In *p*-type superconductors the insulator-metal transitions occur at almost the same carrier densities $x_{IM}=0.06$ and the highest T_c's are achieved at $x=0.16$.[13] On the other hand in *n*-type superconductors the carrier densities of the insulator-metal transitions diverge from $x_{IM}=0.07$ in $Pr_{1-x}LaCe_xCuO_4$ (PLCCO) (Refs. 14–16) to $x_{IM}=0.14$ in NCCO. The carrier density of the highest T_c changes from $x=0.1$ to 0.15 according to materials. In order to extract the physical quantities relating to the insulator-metal transitions, the comparison between materials with different transition carrier densities is useful. In the present Raman scattering experiments NCCO and PLCCO are utilized as the materials with high $x_{IM}=0.14$ and low $x_{IM}=0.07$.

In the present experiments we investigated the carrier density and the temperature dependence of two-phonon Raman scattering in NCCO and PLCCO. The phonon modes with strong electron-phonon interactions change at the insulator-metal transitions and do not change significantly within the metallic phase.

II. TWO-PHONON RAMAN SCATTERING PROCESS

Single-phonon Raman scattering is a third order process: the creation of an electron-hole pair by the absorption of an incident photon, the creation of a phonon by the transition of the electron or the hole, and the creation of a scattered photon by the recombination of the electron-hole pair. The effective two-phonon Raman scattering process is a fourth-order process including twice the phonon creation processes as shown in Fig 1. The intermediate states are virtual states and the energies are not conserved. The two-phonon scattering probability is expressed by,

$$\sigma \propto \left| \sum_{a,b,c} \frac{\langle 0,1|H_{\mathrm{eR}}|0,c\rangle\langle c,n_{j,-k}+1|H_{\mathrm{eL}}|n_{j,-k},b\rangle\langle b,n_{j,k}+1|H_{\mathrm{eL}}|n_{j,k},a\rangle\langle a,n_i-1|H_{\mathrm{eR}}|n_i,0\rangle}{(\omega_c+2\omega_0-\omega_i)(\omega_b+\omega_0-\omega_i)(\omega_a-\omega_i)} \right|^2 \times \delta(\omega_s+2\omega_0-\omega_i), \qquad (2.1)$$

where H_{eR} is the electron-radiation interaction, H_{eL} is the electron-phonon interaction, n_i in the initial state and 1 in the final state are the numbers of incident photons and a scattered photon, $n_{j,k}$ is the number of the j mode at k, 0 in the initial and the final states is the electronic ground state, a, b, and c run over complete sets of intermediate electronic states. The summation includes all the terms for available time orders of interactions.

The intensity of the two-phonon scattering is proportional to the fourth power of the electron-phonon interaction. The two-phonon scattering intensity is usually too small to be detected. However, when the incident photon energy is close to the energy of intermediate electronic state at the resonant Raman condition, the probability of two-phonon Raman scattering as well as single phonon Raman scattering is strongly enhanced. The incident photon energy 2.4 eV in the present experiment is close to the broad charge transfer (CT) energy from the Op band to the Cud upper Hubbard (UH) band. The CT energy increases from 1.5 to 2.2 eV as carrier density increases from $x=0$ to $x=0.17$.[17,18] Therefore the phonon modes vibrating in the CuO_2 plane with strong electron-phonon interactions are selectively enhanced in the two-phonon scattering process.

The two-phonon scattering intensity usually decreases monotonically in many materials as carrier density increases. However, in high T_c superconductors the carrier density dependence is not simple. In high T_c superconductors a sharp quasiparticle band is generated at E_{F} in the metallic phase as calculated by the dynamical mean field theory[19–21] and $1/N$-expansion theory.[22–24] The Raman susceptibility is also calculated in the dynamical mean field theory.[25,26] In Raman scattering of NCCO a sharp quasiparticle band appears at the Fermi energy (E_{F}) in the metallic phase,[27,28] but not in the insulating phase as shown in Fig. 1. In the metallic phase the two-phonon scattering process via the quasiparticle band is added to the process via the original UH band. The UH band is also modified from the insulating phase. Therefore the phonon mode with the strong electron-phonon interaction may be different. The two-phonon scattering intensity is proportional to the sixth power of the intermediate electronic state, if the intermediate states are the similar state. The quasi-particle band shows the strong temperature dependence, sharpening from 300 to 100 K, formation of the pseudogap from 100 K to T_c, and producing the superconducting gap below T_c.[28] If the phonon creation processes occur twice in the quasiparticle band, the scattering intensity is affected by the temperature dependence of the quasiparticle band. If we can detect the correlated temperature dependence between the two-phonon scattering intensity and the electronic density of states of the quasiparticle band, we can conclude that that the observed phonon modes have strong interactions with electrons in the quasiparticle band.

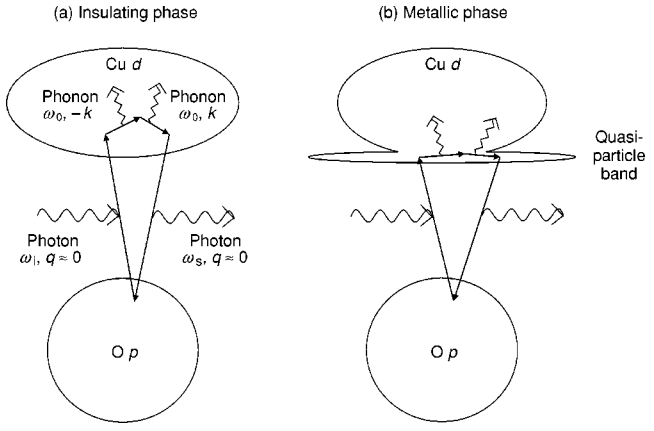

FIG. 1. Resonant two-phonon Raman scattering processes in (a) the insulating phase and (b) the metallic phase. The intermediate states are virtual states and the energies are not conserved. In the metallic phase electrons in the quasiparticle band contribute to the scattering process as intermediate electronic states.

In the single-phonon Raman scattering the momentum of the observable phonon is limited to $k\sim 0$ from the momentum conservation among the phonon, incident photon, and scattered photon. Two types of electron-phonon interactions are known in the single-phonon Raman scattering, one is a short-range interaction like the deformation potential and another is a long-range interaction of the Fröhlich type. Every phonon has the deformation potential-type electron-phonon interaction, while the Fröhlich electron-phonon interaction is limited to the $k\sim 0$ infrared active longitudinal optical (LO) phonons. In the crystal with the inversion symmetry such as NCCO ($I4/mmm$), the Raman active modes are infrared inactive and the infrared active modes are Raman inactive. Sometimes Raman inactive LO modes appear in the A_{1g} Raman spectra by the intraband Fröhlich interaction at the resonant Raman condition.[29,30]

In the two-phonon Raman scattering the restriction of $k\sim 0$ is completely removed, because the creation of phonons at k and $-k$ gives the total excitation of $k=0$. In many cases the two phonons are created in the same phonon branch, and then the two-phonon scattering has the A_{1g} symmetry. The phonon modes observed in the Raman spectra are listed in Table I. In the insulating phase both types of the electron-phonon interactions are participated in the two-phonon Raman scattering.[31,32] On the other hand in the metallic phase doped carriers screen the macroscopic electric field accompanying the LO phonon and the Fröhlich electron-phonon interaction does not work. When the two-phonon peak is comparable or larger then the single-phonon peak, the electron-phonon interaction is anomalously large. This is the case in the two-phonon scattering of high T_c superconductors.

TABLE I. Phonon modes observed in the Raman spectra.

	Single-phonon scattering	Two-phonon scattering
Nonresonant	$A_{1g}+B_{1g}+E_g$ at $k=0$	Weak
Resonant with CT-excitation	$A_{1g}+B_{1g}+E_g+E_u$ (LO) at $k=0$	Strong electron-phonon-interaction modes at any $k+E_u$ (LO) modes at $k=0$

III. EXPERIMENTAL PROCEDURE

Large single crystals were synthesized by a traveling-solvent floating-zone method in an infrared radiation furnace. The undoped crystals of Nd_2CuO_4 were annealed in oxygen gas. Others were annealed in depressurized argon gas from 650 to 890 °C. The $Pr_{1.93}LaCe_{0.07}CuO_4$ crystals were annealed at 800 °C for the antiferromagnetic insulating (AFI) crystals and at 890 °C for the superconducting crystals. The AFI crystal is in the intermediate state between the insulating phase and the metallic phase. The electric resistivity increases below 96 K, but the two-magnon peak energy is much larger than that in the insulating phase of NCCO.[28] The superconducting transition temperatures were determined at the middle points of the transitions on the resistivity curves. The transition temperatures are 25 K ($x=0.14$), 23 K (0.15), 23 K (0.16), and 7 K (0.20) in NCCO and 25 K ($x=0.07$), 27 K (0.1), 25 K (0.15), and 14 K (0.18) in PLCCO. The NCCO crystals at $x=0$, 0.05, and 0.1 are AFI.

Raman spectra were measured in a quasiback scattering configuration utilizing a triple-grating monochromator, a 5145 Å Ar-ion laser, and a cooled charge-coupled device (CCD) detector. A laser beam of 5–20 mW was focused on the 50×500 μm^2 area of cleaved surfaces. The obtained spectra were corrected by the spectroscopic efficiency of the apparatus. Raman spectra were measured in four polarization configurations $(E_i,E_s)=(a,a)$, (a,b), (x,x), and (x,y), where E_i and E_s are the polarizations of incident and scattered light, a and b are parallel to the Cu-O-Cu directions, and x and y are directions rotated by 45° from a and b axes in the ab-plane. The A_{1g} spectra were obtained by the calculation $[(x,x)+(a,a)-(x,y)-(a,b)]/2$.

IV. TWO-PHONON RAMAN SCATTERING IN NCCO

Figure 2 shows the A_{1g} phonon spectra from 5 to 300 K in NCCO. The normal modes of the $k=0$ optical phonons in tetragonal ($I4/mmm$) NCCO are $A_{1g}+B_{1g}+2E_g+3A_{2u}+B_{2u}+4E_u$. Many experimental results of phonon Raman scattering were reported.[33–36] The Raman active modes are A_{1g} (230 cm^{-1} at 30 K), B_{1g} (344 cm^{-1} at 30 K), E_g (126 cm^{-1} at 250 K), and E_g (494 cm^{-1} at 30 K) in Nd_2CuO_4.[33,35] The A_{1g} mode has large scattering intensity in the (c,c) spectra, because this mode is the c-axis vibration of Nd atoms. The peaks from about 700 to 1200 cm^{-1} are caused by two-phonon scattering. At $x=0$ the largest peak is the A peak (1168 cm^{-1}) the second largest peak is the B peak (1029 cm^{-1}). As Ce concentration increases, the A peak decreases in energy and intensity in the insulating phase and becomes the smallest peak among the A, B', C, and D peaks in the metallic phase. On the other hand the B peak increases in intensity and becomes the largest B' peak in the metallic phase. The energy of the B' peak is 975 cm^{-1} at $x=0.16$. In the metallic phase the second largest peak is the D peak (816 cm^{-1}) and the next is the C peak (906 cm^{-1}).

The peak energies and the intensities are plotted in Fig. 3. The areas of the circles are proportional to the scattering intensities of decomposed Gaussian peaks. The 1168 cm^{-1} A peak at $x=0$ decreases gradually in energy and intensity, as carrier density increases in the AFI phase. Then the intensity decreases suddenly at the insulator-metal transition from $x=0.1$ to $x=0.14$. The small 1029 cm^{-1} B peak at $x=0$ increases in intensity as carrier density increases, and becomes the most dominant B' peak in the metallic phase.

The neutron scattering experiment of the phonon density of states disclosed that the 573 cm^{-1} ($x=0$) peak decreases in energy and intensity as carrier density increases from $x=0$ to $x=0.08$, but the 540 cm^{-1} ($x=0$) peak retains the intensity into the metallic phase.[37] It is consistent with our results of the A and $B+B'$ modes.

In order to find out the phonon modes of the two-phonon peaks, first let us check whether the phonon modes are the $k=0$ modes or the $k>0$ modes. The Raman active single-phonon modes (A_{1g}, B_{1g}, and E_g) and infrared active single-phonon modes (A_{2u} and E_u) are the $k=0$ modes. All the energies of the two-phonon peaks are different from twice the energies of the single-phonon Raman active modes. Therefore the two-phonon peaks do not come from the Raman active phonons at $k=0$. The energies of the LO phonons were measured by infrared spectroscopy.[34,38,39] The LO phonon energies are higher than the transverse optical (TO) phonon energies by the restoring forces of the macroscopic electric fields accompanying the LO phonons. The TO (LO) phonon energies of the infrared active modes in Nd_2CuO_4 are 134 (144), 282 (433), and 516 (559) cm^{-1} for the A_{2u} modes, 132 (139), 304 (341), 353 (432), and 512 (593) cm^{-1} for the E_u modes at 10 K.[34] The oscillator strengths of the infrared-active phonons are proportional to the square of macroscopic electric fields of the LO phonons.

Figure 4 shows the comparison between the single-phonon spectra and the two-phonon spectra at 5 and 300 K. Note that the energy range for the single-phonon spectra is 300–650 cm^{-1}, and the energy range for the two-phonon spectra is 600–1300 cm^{-1}. The LO phonon energies at $k=0$ observed by infrared spectroscopy are shown by the arrows. The peak energies 559 and 592 cm^{-1} in the single-phonon spectra are close to the LO phonon energies of the 559 cm^{-1} A_{2u} mode and the 593 cm^{-1} E_u mode at $x=0$. These single-phonon Raman peaks are probably induced by the intraband Fröhlich interaction at the resonant Raman condition.[29] The largest two-phonon peak energy 1168 cm^{-1} is a little differ-

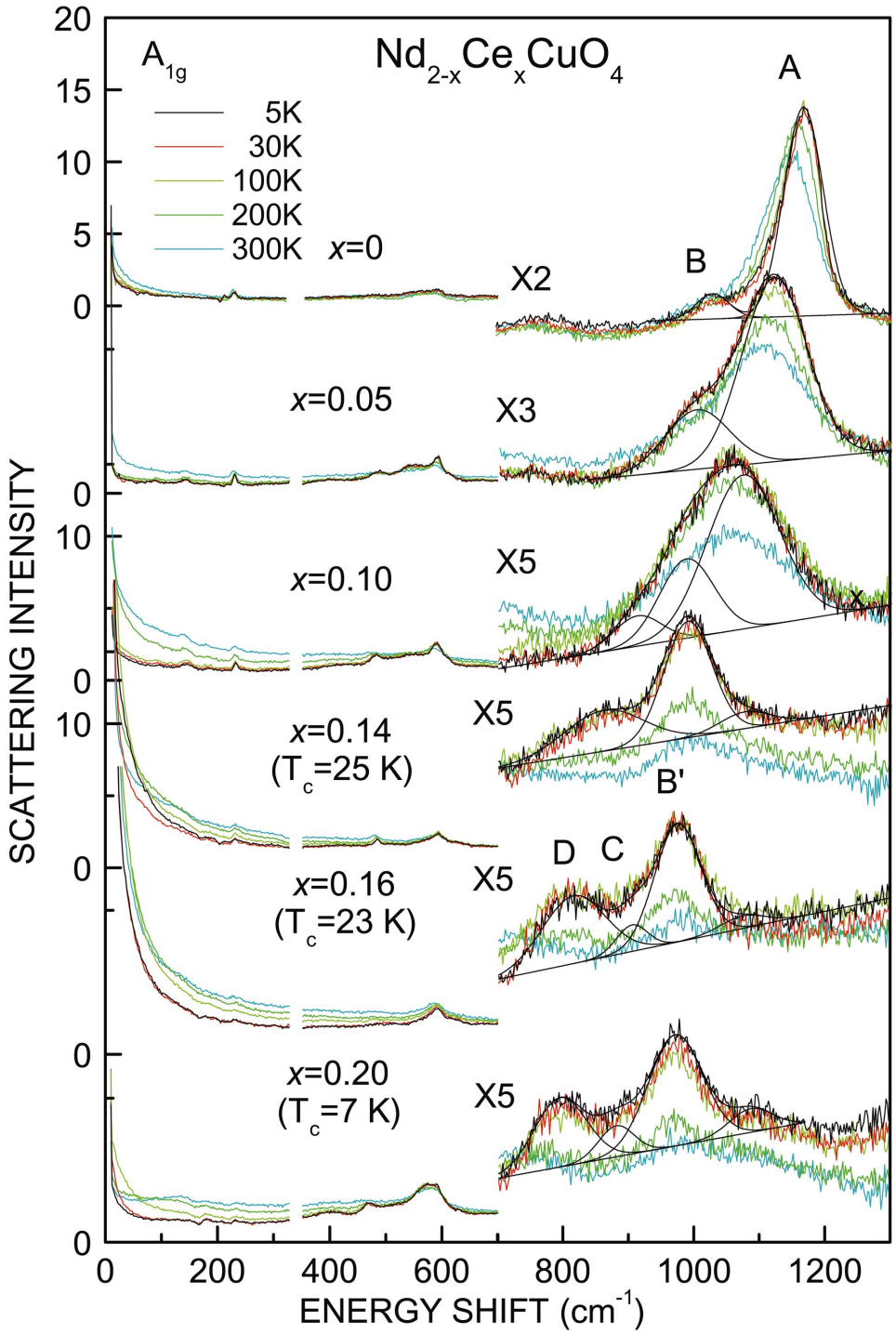

FIG. 2. (color) A_{1g} scattering spectra in NCCO. The two-phonon scattering peaks at 5 K are decomposed into Gaussian peaks.

ent from twice the LO phonon energies 559×2 cm^{-1} and 593×2 cm^{-1}. The two-phonon peak energy decreases from 1168 to 1148 cm^{-1}, as temperature increases from 5 to 300 K. If the origin of the two-phonon peak is the $k=0$ phonon observed in the single-phonon scattering, the single-phonon peak energy should decrease by $(1168-1148)/2=10$ cm^{-1}. Such energy shift of the single-phonon peak is not observed. Therefore the 1168 cm^{-1} (5 K) two-phonon peak is not the Raman active modes nor the infrared active modes at $k=0$. Two-phonon peak energy decreases from 1168 cm^{-1} at $x=0$ to 1076 cm^{-1} at $x=0.1$ and 1091 cm^{-1} at $x=0.2$. On the other hand the energies of the single-phonon peaks at 559 and 592 cm^{-1} at $x=0$ are little changed from $x=0$ to 0.1 and 0.2 as shown in Figs. 2 and 4. This result again indicates that the 559 and 592 cm^{-1} peaks are not the origin of the 1168 cm^{-1} ($x=0$) two-phonon peak.

In $Nd_{1.8}Ce_{0.2}CuO_4$ the two-phonon peaks at 890, 972, and 1090 cm^{-1} have not the corresponding single-phonon peaks. The energy of the 796 cm^{-1} two-phonon peak is near twice the energy of the 403 cm^{-1} single-phonon peak at 5 K, but the temperature dependence is different. The 796 cm^{-1} two-phonon peak at 5 K decreases to 749 cm^{-1} as temperature

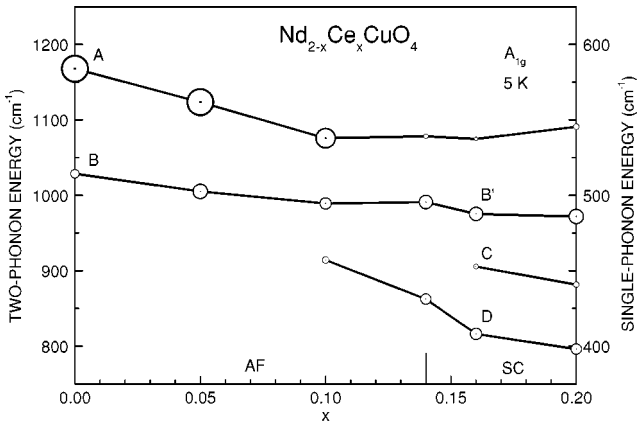

FIG. 3. Energies of two-phonon peaks at 5 K. The areas of circles are proportional to integrated scattering intensities of the peaks.

increases to 300 K. Whereas the 403 cm^{-1} single-phonon peak at 5 K little shift as temperature increases to 300 K. Therefore the 403 cm^{-1} single-phonon mode at 5 K is not the origin of the 796 cm^{-1} two-phonon peak at 5 K. These results indicate that the origins of the two-phonon Raman peaks are not the $k=0$ modes.

Next the two-phonon peaks are compared with large k-modes. Figure 5 shows phonon dispersion curves of the Σ_1 modes along (π,π) and the Δ_1 modes along $(\pi,0)$ at $x=0$

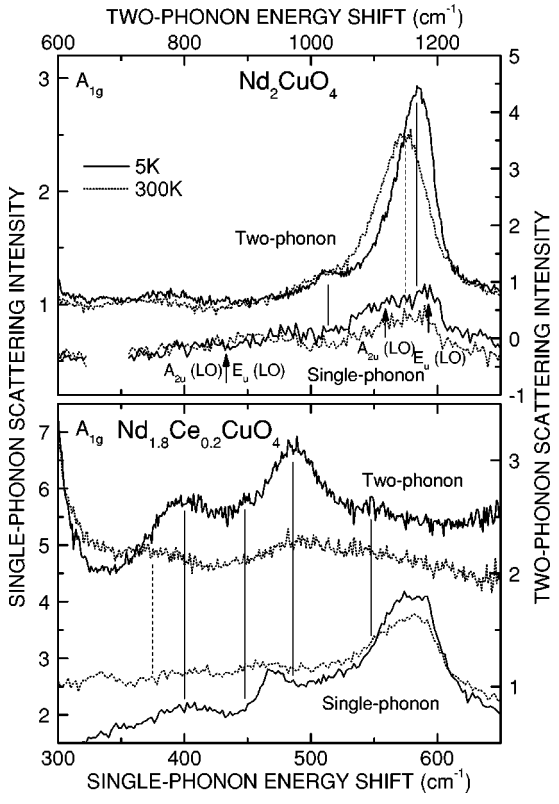

FIG. 4. Comparison between the two-phonon scattering peaks and the single-phonon scattering peaks. The energies of the 5 K two-phonon peaks are indicated by solid lines and the 300 K peak by dotted lines. The energies of the LO modes measured by infrared spectroscopy are shown by arrows.

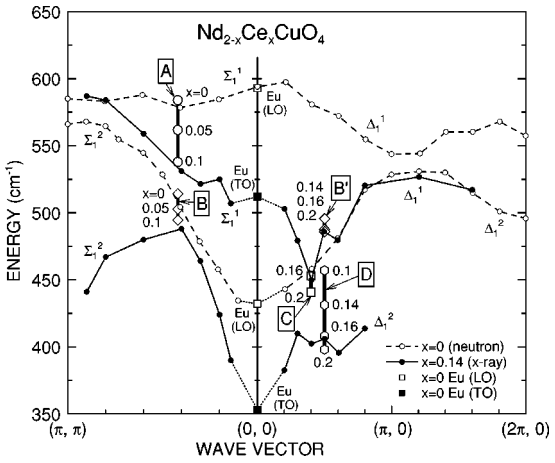

FIG. 5. The phonon modes with large two-phonon scattering intensities are mapped into the phonon dispersion curves measured by neutron scattering (Ref. 4) at $x=0$ and by inelastic x-ray scattering (Refs. 9 and 10) at $x=0.14$. The experimental points are connected by us for the x-ray scattering. The TO and LO E_u modes at $x=0$ measured by infrared spectroscopy (Ref. 34) are also shown. The A and B two-phonon peaks in the insulating phase are assigned to the Σ_1^1 mode and the Σ_1^2 mode around $(0.42\pi,0.42\pi)$. The B', C, and D peaks in the metallic phase are assigned to the Δ_1^1 mode around $(0.4\pi,0)$, Δ_1^1 mode around $(0.5\pi,0)$, and Δ_1^2 mode around $(0.5\pi,0)$.

measured by neutron scattering[4] and at $x=0.14$ measured by inelastic x-ray scattering.[9,10] The highest-energy mode is the Cu-O(1) bond-stretching longitudinal mode and the second highest-energy mode is mainly associated with the O(2) vibrating longitudinal mode.[9] The E_u infrared active phonon modes in the insulating phase $x=0$ at (0,0) are also shown by the open squares (LO) and the solid squares (TO).[34] The Σ_1 modes and the Δ_1 modes become the E_u (LO) modes at (0,0), because the Σ_1 modes and the Δ_1 modes are longitudinal modes. At $x=0$ the Σ_1 modes and the Δ_1 modes are smoothly connected to the E_u (LO) modes at (0,0) as expected. The Σ_1 modes and the Δ_1 modes at $x=0.14$ are connected to the E_u (TO) modes at $x=0$. It indicates that the macroscopic electric fields accompanying the LO modes are almost completely screened by doped carriers at $x=0.14$ and the energies of the LO phonons approach the energies of the TO phonons. The Δ_1^1 mode at $x=0.14$ strongly softens at $(0.4\pi,0)$. The Δ_1^2 mode at $x=0.14$ also strongly softens from $(0.4\pi,0)$ to $(0.6\pi,0)$.

The energy of the strongest two-phonon A peak decreases from 1168 cm^{-1} at $x=0$ to 1076 cm^{-1} at $x=0.1$ in the insulating phase. The corresponding single-phonon energy decreases from 584 to 538 cm^{-1}. This phonon mode is uniquely determined to be the Σ_1^1 mode near $(0.42\pi,0.42\pi)$ from the coincidence of the energy as shown in Fig. 5. The energy of the second strongest B peak decreases from 1029 cm^{-1} at $x=0$ to 989 cm^{-1} at $x=0.1$. The corresponding energy shift is observed in the Σ_1^2 mode near $(0.42\pi,0.42\pi)$. In the metallic phase the second largest D peak decreases from 914 cm^{-1} at $x=0.1$ to 796 cm^{-1} at $x=0.2$. The corresponding energy shift is uniquely observed in the Δ_1^2 mode at $x=0.14$ near $(0.5\pi,0)$. The small C peak shifts from 906 cm^{-1} at x

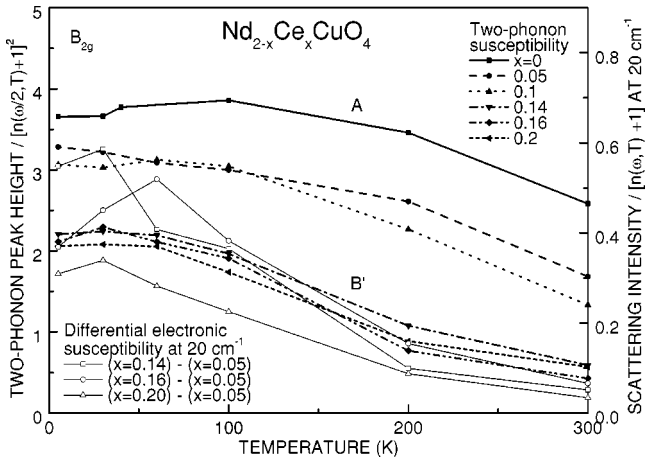

FIG. 6. Temperature dependences of two-phonon scattering susceptibilities $[I(\text{peakheight})/[n(\omega/2,T)+1]^2]$ of the decomposed Gaussian A peaks in the insulating phase and the B' peak in the metallic phase (thick lines). The temperature dependences of the differential electronic susceptibilities $\{I(\text{scatteringintensity})/[n(\omega,T)+1]\}$ at 20 cm^{-1} between the metallic phases and the insulating phase $x=0.05$. They give the measure of the electronic density of states in the quasiparticle band at E_F.

$=0.16$ to 882 cm^{-1} at $x=0.2$. The energy corresponds to the sharp dip of the Δ_1^1 mode at $(0.4\pi,0)$ in the metallic phase $x=0.14$. The B peak in the insulating phase becomes the strongest B' peak in the metallic phase. The energy decreases from 991 cm^{-1} at $x=0.14$ to 972 cm^{-1} at $x=0.2$. The corresponding energy is observed both in the Σ_1^2 mode at $(0.4\pi,0.4\pi)$ and in the Δ_1^1 mode at $(0.5\pi,0)$. Both modes can be distinguished from the temperature dependence of the scattering intensity. The peak height decreases to 43% in the insulating phase $x=0.1$ as temperature increases from 5 to 300 K, while the peak height rapidly decreases to 27% in the metallic phase $x=0.14$. The temperature dependence in the metallic phase is the same as C and that of the D modes. Therefore the B' mode in the metallic phase is assigned to the Δ_1^1 mode at $(0.5\pi,0)$ differently from the B mode in the insulating phase. The different temperature dependence between the insulating phase and the metallic phase is interpreted by the growing up of the quasi-particle band in the metallic phase as temperature decreases.

Figure 6 shows the temperature dependence of the Raman susceptibility of the two-phonon A peak in the insulating phase and the B' peak in the metallic phase. The Raman susceptibility is obtained by $\chi(\omega,T)=I_{\text{two-phonon}}(\omega,T)/[n(\omega/2,T)+1]^2$. In the insulating phase the height of the A peak decreases to 70% at $x=0$, 50% at $x=0.05$, and 43% at $x=0.1$. The decreasing rate is that of the usual two-phonon scattering. While in the metallic phase the B'-peak height decreases to 27% at $x=0.14$, 20% at $x=0.16$, and 28% at $x=0.2$. In the insulating phase the decreasing rate increases gradually from 100 to 300 K. While in the metallic phase it increases from 30 to 200 K and decreases to 300 K. It is expected that the difference is caused by the appearance of the quasiparticle band in the metallic phase as shown in Fig. 1.

In the metallic phase doped carriers form a quasiparticle band with the width of about 800 cm^{-1} at E_F.[27,28] The quasiparticle band sharpens to form a narrow resonant peak at E_F as temperature decreases from 300 to 100 K. The width at half maximum is about 50 cm^{-1} in $Nd_{1.86}Ce_{0.14}CuO_4$ at 100 K. The pseudogap of about 150 cm^{-1} is formed at E_F as temperature decreases from 100 K to T_c. Below T_c the superconducting gap is produced. The sharpening of the quasiparticle band and the formation of the pseudogap are stronger in the B_{2g} symmetry than in the B_{1g} symmetry.

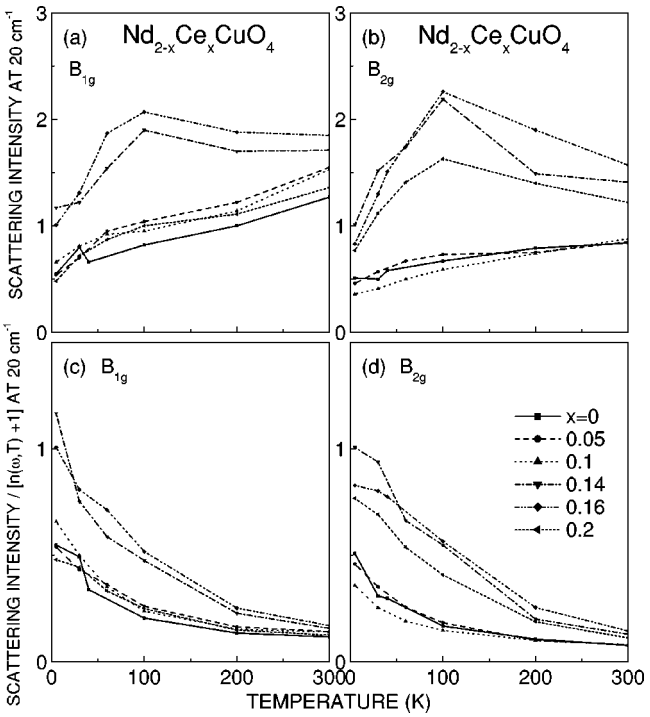

FIG. 7. Temperature dependences of the electronic scattering intensities at 20 cm^{-1} in (a) B_{1g} and (b) B_{2g}, and the susceptibilities $\{I(\text{scatteringintensity})/[n(\omega,T)+1]\}$ in (c) B_{1g} and (d) B_{2g}.

Figure 7 shows the temperature dependence of the low-energy scattering intensity at 20 cm^{-1}. This scattering comes from the electronic excitation of 20 cm^{-1} near E_F in the quasiparticle band. Figures 7(a) and 7(b) show the observed intensities in the B_{1g} and B_{2g} spectra, respectively. These are the same as our previous paper.[28] The B_{1g} intensity at $x=0.16$ is reduced by 0.8 which is the estimated background level at 20 cm^{-1}, because the spectra include a little large elastically scattered light. The intensity of the small peak due to the spin wave of the Nd-Cu mixed mode is removed. The clear difference between the insulating phase and the metallic phase is observed except for $x=0.2$ in B_{1g}. In the insulating phase the scattering intensity is small and decreases monotonically as temperature decreases at $x=0$, 0.05, and 0.1. On the other hand in the metallic phase the scattering intensity increases from 300 to 100 K and decreases below 100 K at $x=0.14$ and 0.16 in B_{1g} spectra and at $x=0.14$, 0.16, and 0.2 in B_{2g} spectra. This temperature dependence is caused by the sharpening of the quasiparticle band from 300 to 100 K and the formation of the pseudo-gap below 100 K. The increase of the scattering intensity at 100 K is larger in B_{2g} than in B_{1g}. The B_{1g} scattering intensity at $x=0.2$ shows the similar temperature dependence as that in the insulating phase, which indicates that the quasiparticle band is weak.

The B_{1g} and B_{2g} Raman susceptibilities $\chi(\omega) = I(\omega)/[n(\omega,T)+1]$ are shown in Figs. 7(c) and 7(d), respectively. In this expression the susceptibility increases as temperature decreases. The effect of the pseudo-gap below 100 K observed in Figs. 7(a) and 7(b) are changed into the decrease of the increasing speed of the susceptibility below 100 K. The difference between the metallic phase and the insulating phase is caused by the presence and absence of the quasiparticle band.

The B_{2g} differential electronic Raman susceptibilities between the metallic phase and the insulating phase ($x=0.05$) at 20 cm^{-1} are plotted by thin lines in Fig. 6. The differential susceptibility is caused by the formation of the quasiparticle band near $(\pi/2,\pi/2)$. It is clearly shown that the susceptibility of the two-phonon B' peak in the metallic phase has similar temperature dependence to the differential electronic susceptibility. The susceptibility of the two-phonon A peak has different temperature dependence from the electronic susceptibility of the quasiparticle band. In the insulating phase the B peak has the similar temperature dependence to the A peak. On the other hand in the metallic phase the C and D peaks have similar temperature dependence to the B' peak. This is the reason that the B' peak is assigned to the Δ_1^1 mode near $(0.5\pi,0)$ rather than the Σ_1^2 mode near $(0.42\pi,0.42\pi)$.

V. TWO-PHONON RAMAN SCATTERING IN PLCCO

Figure 8 shows the A_{1g} phonon spectra from 5 to 300 K in PLCCO. In Pr_2CuO_4 the energies of Raman active phonon modes are A_{1g} (233 cm^{-1}), B_{1g} (287 cm^{-1}), E_g (165 and 474 cm^{-1}) at 30 K (Ref. 40) and those of the TO (LO) infrared active modes are A_{2u}, [135 (147), 271 (428), and 505 (552) cm^{-1}], E_u [124 (130), 300 (330), 336 (430), and 486 (576) cm^{-1}] at 10 K.[41] In PLCCO the broad two-phonon peak at 1103 cm^{-1} ($x=0.07$) in the insulating phase corresponds to the broad two-phonon A peak at $x=0.1$ in NCCO. The largest peak at 917 cm^{-1} in the metallic phase at $x=0.15$ corresponds to the 975 cm^{-1} B' peak in the metallic phase at $x=0.16$ in NCCO as shown in Fig. 2. Therefore it indicates that the change of the phonon modes with the strong electron-phonon interactions occurs at the insulator-metal transition, not at the fixed carrier density.

The peak energies and the intensities are plotted in Fig. 9. The areas of the circles are proportional to the scattering intensities for the modes. The A peak decreases in intensity as carrier density increases, although the change is slow compared with NCCO. The B' peak is the most dominant peak in the metallic phase.

VI. COMPARISON WITH *P*-TYPE HIGH T_C SUPERCONDUCTORS

In p-type high T_c superconductors the shift of the strong electron-phonon-interaction mode in k-space seems to help the shift of the superconducting coherent peak as carrier density increases. In the p-type high T_c superconductors the coherent peak is stronger around $(\pi/2,\pi/2)$ than around $(\pi,0)$ at low carrier densities, but the position of the stronger coherent peak is exchanged at high carrier densities.[11] The crossover occurs at the carrier density of the highest T_c in $La_{2-x}Sr_xCuO_4$ (LSCO) and the 60 K phase in $YBa_2Cu_3O_y$ (YBCO). In $Bi_2Sr_2Ca_{1-x}Y_xCu_2O_{8+\delta}$ (Bi2212) the coherent peak is observed at both $(\pi/2,\pi/2)$ and $(\pi,0)$ from underdoping to overdoping, but the stronger coherent peak changes from $(\pi/2,\pi/2)$ to $(\pi,0)$ at the optimum doping. In $Bi_2Sr_{2-x}La_xCuO_{6+\delta}$ and $Bi_{1.74}Pb_{0.38}Sr_{1.88}CuO_{6+\delta}$ (Bi2201) the coherent peak at $(\pi/2,\pi/2)$ decreases in intensity from the underdoped phase to the optimally doped phase and disappears in the overdoped phase. The coherent peak at $(\pi,0)$ increases in intensity as carrier density increases. This change of the coherent peak in k-space is correlated with the change in the electronic density of states near E_F from $(\pi/2,\pi/2)$ to $(\pi,0)$, but the proportionality relation is not satisfied.

Low-energy electronic Raman scattering can be assigned to the intraband excitations in the quasiparticle band which is generated by the strongly correlated-electron effects at E_F. The electronic density of states around $(\pi/2,\pi/2)$ increases rapidly from the undoped insulating phase to the insulator-metal transition point and then decreases gradually as carrier density increases.[11] On the other hand the electronic density of states around $(\pi,0)$ increases gradually as carrier density increases. The intensity crossing occurs near the optimum carrier density in LSCO, Bi2212, and Bi2201, and the 60 K phase in YBCO. The crossing of the coherent peak from $(\pi/2,\pi/2)$ to $(\pi,0)$ occurs in the narrow carrier density region, but the transfer of the electronic density of states from $(\pi/2,\pi/2)$ to $(\pi,0)$ is gradual with the increase of the carrier density. Therefore an additional mechanism is necessary to accelerate the change in the coherent peak position in k-space.

In the previous paper[11] our group reported that the phonon mode of the largest two-phonon scattering peak changes from the breathing mode at (π,π) to the half breathing mode at $(\pi,0)$ in correlation with the change of the coherent peak from $(\pi/2,\pi/2)$ to $(\pi,0)$. It is calculated that the half-breathing Δ_1 mode at $(\pi,0)$ modulate the magnetic excitation-mediated superconductivity to enhance the pairing.[2,12] The change of the phonon mode with the strongest electron-phonon interaction accelerates the change of the position of the coherent peak in k-space.

In n-type high T_c superconductors the carrier density dependence of the large electronic density of states in k-space is opposite to the p-type high T_c superconductors. In NCCO, angle-resolved photoemission spectroscopy (ARPES) disclosed that doped carriers enter only around $(\pi,0)$ in the insulating phase.[42–44] The density of states around $(\pi/2,\pi/2)$ increases after the phase changes into the metal. The density of states at $(0.35\pi,0.6\pi)$ are kept depleted. The low-energy electronic Raman scattering is consistent with the results of ARPES.[27,28] Raman scattering experiment disclosed that a quasiparticle band is formed below 800 cm^{-1} at 300 K only in the metallic phase. It sharpens to the width of about 50 cm^{-1} as temperature decreases to 100 K, the low-energy part decreases in intensity to form the pseudogap below 100 K, and the superconducting coherent peak is produced below T_c.[28] The superconducting coherent peak is observed both around $(\pi/2,\pi/2)$ and $(\pi,0)$ and no crossover is observed.[28,45,46]

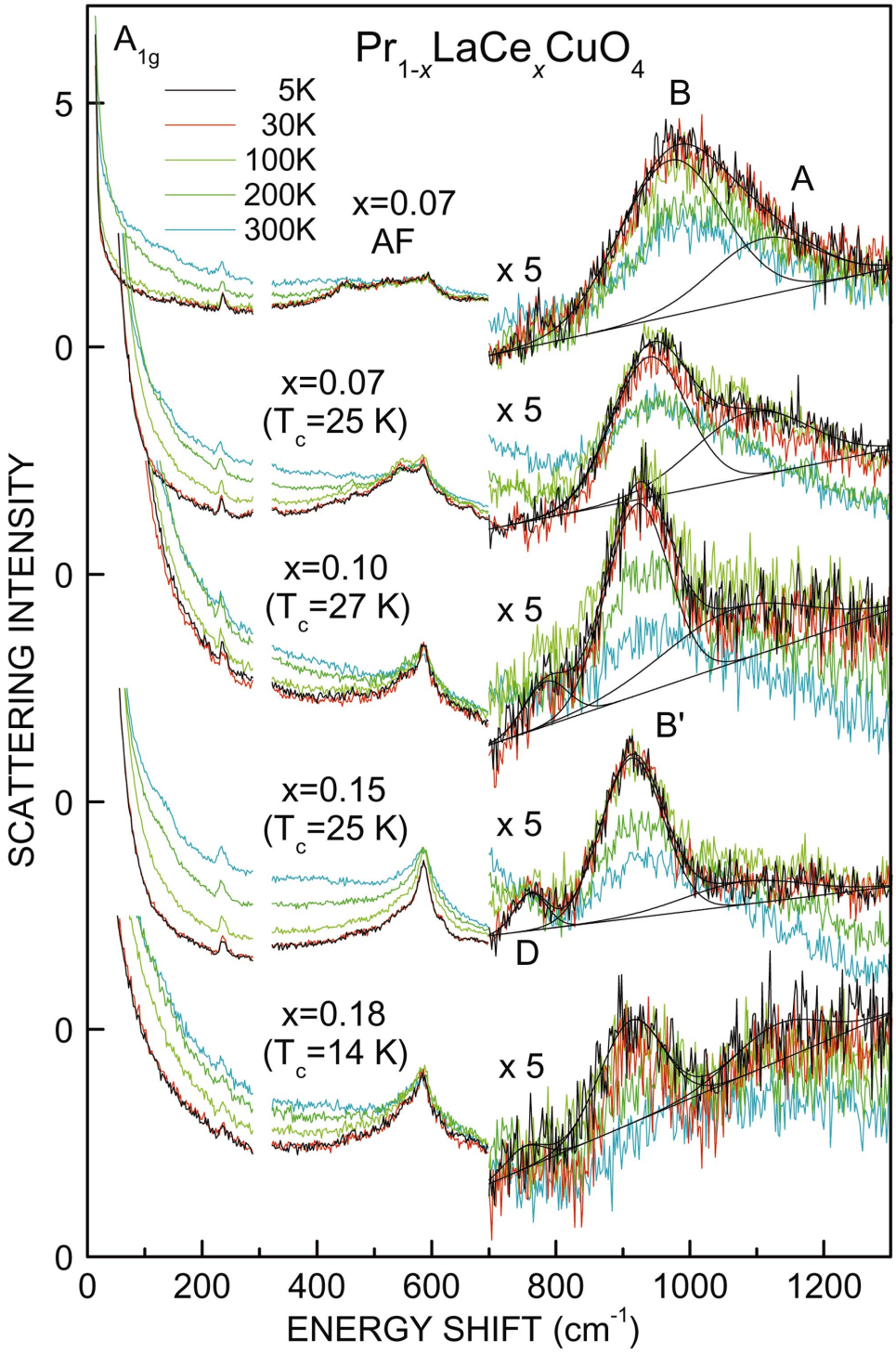

FIG. 8. (color) A_{1g} scattering spectra in PLCCO. The two-phonon scattering peaks at 5 K are decomposed into Gaussian peaks.

In *n*-type superconductors the strong contribution of the phonon mode at $(\pi,0)$ to the pair creation is not predicted.[2,12] In fact the strong electron-phonon interactions occur around $(0.4\pi,0)$ in the metallic phase. The wave vector for the strong electron-phonon interactions sharply changes from around $(0.4\pi,0.4\pi)$ to around $(0.4\pi,0)$ at the insulator-metal transition but does not change in the metallic phase. It is related to the superconducting properties in *n*-type high T_c superconductors that the highest T_c occurs near the insulator-metal transition and the intensity ratio between the superconducting coherent peaks at $(\pi/2,\pi/2)$ and $(\pi,0)$ little depends on the carrier density.

The position of the strong electron-phonon interaction and the position of the large electronic density of states near E_F are shown in Fig. 10. The clear correlation is observed between the change of the strong electron-phonon-interaction mode and that of the large electronic density of states. The change of the phonon modes is caused by the change of the electronic states. Inversely it is supposed that the electron-phonon interaction affects to generate the electronic states. In

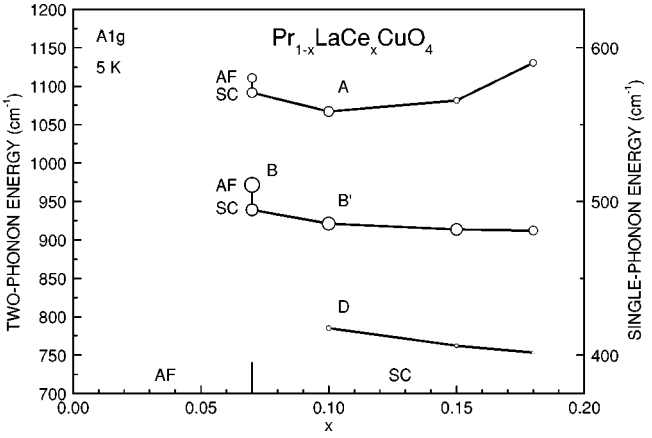

FIG. 9. Energies of two-phonon peaks at 5 K. The areas of circles are proportional to integrated scattering intensities of the peaks.

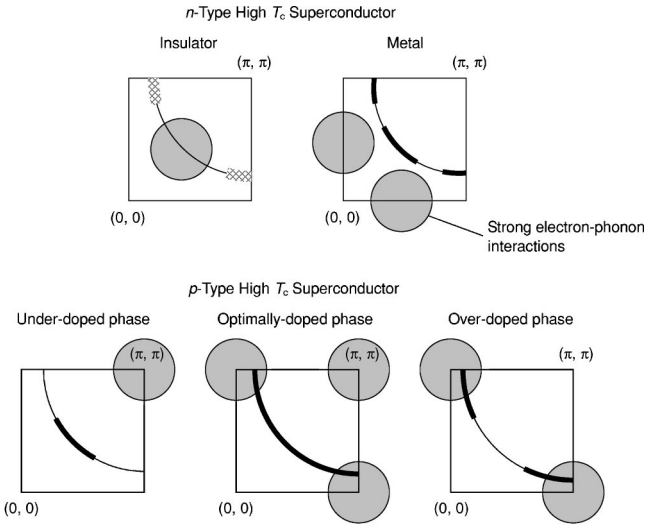

FIG. 10. The positions of the large electronic density of states at E_F (hatched curves in the insulating phase and thick curves in the metallic phases) and the large electron-phonon interactions (gray circles).

the insulating phase the wave vector of the strong electron-phonon interaction mode corresponds to the wave vector of the depleted Fermi surface near $(\pi/2, \pi/2)$. The position of doped electrons in *k*-space $(\pi, 0)$ can be derived from the electronic properties alone,[47] but it is difficult to explain the insulating properties to $x=0.14$. The electron-phonon interaction seems to contribute to form the wide insulating phase from $x=0$ to 0.14 in NCCO. In the metallic phase the wave vector of the strong electron-phonon interaction mode corresponds to the wave vector connecting the two Fermi surfaces near $(\pi, \pi/4)$ and $(\pi, -\pi/4)$. The electronic state may include the phonon component.

VII. CONCLUSIONS

The strong electron-phonon-interaction modes are determined from the two-phonon Raman scattering. The modes change from the Σ_1 modes near $(0.4\pi, 0.4\pi)$, 584 and 514 cm^{-1} at $x=0$, to the Δ_1 modes near $(0.4\pi, 0)$, 488, 453, and 408 cm^{-1} $(x=0.16)$ in NCCO. The similar change is also observed at the insulator-metal transition in PLCCO. The change occurs at the insulator-metal transition and does not occur in the metallic phase. It is different from the *p*-type high T_c superconductors in which the strongest electron-phonon-interaction mode changes from the breathing mode at (π, π) in the low-doping phase to the half-breathing mode at $(\pi, 0)$ in the high-doping phase. The temperature dependence of the two-phonon peak abruptly changes at the insulator-metal transition. The difference of the electronic states in the insulating phase and the metallic phase is the absence and the presence of the quasiparticle band at E_F, respectively. The temperature dependence of the two-phonon peak in the metallic phase is the same as that of the electronic Raman susceptibility of the quasiparticle band. Therefore we conclude that the observed two-phonon modes in the metallic phase have strong electron-phonon interactions with electrons in the quasiparticle band.

[1] T. Valla, A. V. Fedorov, P. D. Johnson, B. O. Wells, S. L. Hulbert, Q. Li, G. D. Gu, and N. Koshizuka, Science **285**, 2110 (1999).
[2] Z.-X. Shen, A. Lanzara, S. Ishihara, and N. Nagaosa, Philos. Mag. B **82**, 1349 (2002).
[3] A. Lanzara, P. V. Bogdanov, X. J. Zhou, S. A. Kellar, D. L. Feng, E. D. Lu, T. Yoshida, H. Eisaki, A. Fujimori, K. Kishio, J.-I. Shimoyama, T. Noda, S. Uchida, Z. Hussain, and Z.-X. Shen, Nature (London) **412**, 510 (2001).
[4] L. Pintschovius, N. Pyka, W. Reichardt, A. Y. Rumiantsev, N. L. Mitrofanov, A. S. Ivanov, G. Collin, and P. Bourges, Physica C **185–189**, 156 (1991).
[5] L. Pintschovius and W. Reichardt, in *Physical Properties of High Temperature Superconductors IV*, edited by P. Ginsberg (World Scientific, Singapore 1995), p. 295.
[6] R. J. McQueeney, Y. Petrov, T. Egami, M. Yethiraj, G. Shirane, and Y. Endoh, Phys. Rev. Lett. **82**, 628 (1999).
[7] L. Pintschovius and M. Braden, Phys. Rev. B **60**, R15039 (1999).
[8] R. J. McQueeney, J. L. Sarrao, P. G. Pagliuso, P. W. Stephens, and R. Osborn, Phys. Rev. Lett. **87**, 077001 (2001).
[9] M. d'Astuto, P. K. Mang, P. Giura, A. Shukla, P. Ghigna, A. Mirone, M. Braden, M. Greven, M. Krisch, and F. Sette, Phys. Rev. Lett. **88**, 167002 (2002).
[10] M. d'Astuto, P. K. Mang, P. Giura, A. Shukla, A. Mirone, M. Krisch, F. Sette, P. Ghigna, M. Braden, and M. Greven, Int. J. Mod. Phys. B **17**, 484 (2003).
[11] S. Sugai, H. Suzuki, Y. Takayanagi, T. Hosokawa, and N. Hayamizu, Phys. Rev. B **68**, 184504 (2003).
[12] S. Ishihara and N. Nagaosa, Phys. Rev. B **69**, 144520 (2004).
[13] J. L. Tallon, C. Bernhard, H. Shaked, R. L. Hitterman, and J. D. Jorgensen, Phys. Rev. B **51**, 12911 (1995).
[14] Y. Koike, A. Kakimoto, M. Mochida, H. Sato, T. Noji, M. Kato, and Y. Saito, Jpn. J. Appl. Phys., Part 1 **31**, 2721 (1992).

[15] J. L. García-Muñoz, M. Suaaidi, J. Fontcuberta, S. Piñol, and X. Obradors, Physica C **268**, 173 (1996).
[16] M. Fujita, T. Kubo, S. Kuroshima, T. Uefuji, K. Kawashima, K. Yamada, I. Watanabe, and K. Nagamine, Phys. Rev. B **67**, 014514 (2003).
[17] Y. Tokura, S. Koshihara, T. Arima, H. Takagi, S. Ishibashi, T. Ido, and S. Uchida, Phys. Rev. B **41**, 11657 (1990).
[18] S. Uchida, T. Ido, H. Takagi, T. Arima, Y. Tokura, and S. Tajima, Phys. Rev. B **43**, 7942 (1991).
[19] A. Georges, G. Kotliar, W. Krauth, and M. J. Rozenberg, Rev. Mod. Phys. **68**, 13 (1996).
[20] M. Imada, A. Fujimori, and Y. Tokura, Rev. Mod. Phys. **70**, 1039 (1998).
[21] X. Y. Zhang, M. J. Rozenberg, and G. Kotliar, Phys. Rev. Lett. **70**, 1666 (1993).
[22] H. Jichu, T. Matsuura, and Y. Kuroda, J. Phys. Soc. Jpn. **59**, 2820 (1990).
[23] Y. Ōno, T. Matsuura, and Y. Kuroda, J. Phys. Soc. Jpn. **64**, 1595 (1995).
[24] T. Arimoto, T. Ohara, A. Tsuruta, A. Kobayashi, and Y. Kuroda, J. Phys. Soc. Jpn. **72**, 904 (2003).
[25] J. K. Freericks and T. P. Devereaux, Phys. Rev. B **64**, 125110 (2001).
[26] J. K. Freericks, T. P. Devereaux, R. Bulla, and Th. Pruschke, Phys. Rev. B **67**, 155102 (2003).
[27] A. Koitzsch, G. Blumberg, A. Gozar, B. S. Dennis, P. Fournier, and R. L. Greene, Phys. Rev. B **67**, 184522 (2003).
[28] S. Sugai, Y. Sone, and H. Mabuchi (unpublished).
[29] R. M. Martin, Phys. Rev. B **4**, 3676 (1971).
[30] E. T. Heyen, J. Kircher, and M. Cardona, Phys. Rev. B **45**, 3037 (1992).
[31] M. Yoshida, S. Tajima, N. Koshizuka, S. Tanaka, S. Uchida, and T. Itoh, Phys. Rev. B **46**, 6505 (1992).
[32] M. Reedyk, C. Thomsen, M. Cardona, J. S. Xue, and J. E. Greedan, Phys. Rev. B **50**, 13762 (1994).
[33] S. Sugai, T. Kobayashi, and Jun Akimitsu, Phys. Rev. B **40**, 2686 (1989).
[34] E. T. Heyen, G. Kliche, W. Kress, W. König, M. Cardona, E. Rampf, J. Prade, U. Schröder, A. D. Kulkarni, F. W. de Wette, S. Piñol, D. McK. Paul, E. Morán, and M. A. Alario-Franco, Solid State Commun. **74**, 1299 (1990).
[35] Z. V. Popovic, A. Sacuto, and M. Balkanski, Solid State Commun. **78**, 99 (1991).
[36] E. T. Heyen, R. Liu, M. Cardona, S. Piñol, R. J. Melville, D. McK. Paul, E. Morán, and M. A. Alario-Franco, Phys. Rev. B **43**, 2857 (1991).
[37] H. J. Kang, Pengcheng Dai, D. Mandrus, R. Jin, H. A. Mook, D. T. Adroja, S. M. Bennington, S.-H. Lee, and J. W. Lynn, Phys. Rev. B **66**, 064506 (2002).
[38] M. K. Crawford, G. Burns, G. V. Chandrashekhar, F. H. Dacol, W. E. Farneth, E. M. McCarron III, and R. J. Smalley, Phys. Rev. B **41**, 8933 (1990).
[39] C. C. Homes, B. P. Clayman, J. L. Peng, and R. L. Greene, Phys. Rev. B **56**, 5525 (1997).
[40] S. Sugai, T. Kobayashi, and J. Akimitsu, Solid State Commun. **74**, 599 (1990).
[41] M. K. Crawford, G. Burns, G. V. Chandrashekhar, F. H. Dacol, W. E. Farneth, E. M. McCarron III, and R. J. Smalley, Solid State Commun. **73**, 507 (1990).
[42] N. P. Armitage, D. H. Lu, D. L. Feng, C. Kim, A. Damascelli, K. M. Shen, F. Ronning, Z.-X. Shen, Y. Onose, Y. Taguchi, and Y. Tokura, Phys. Rev. Lett. **86**, 1126 (2001).
[43] N. P. Armitage, D. H. Lu, C. Kim, A. Damascelli, K. M. Shen, F. Ronning, D. L. Feng, P. Bogdanov, Z.-X. Shen, Y. Onose, Y. Taguchi, Y. Tokura, P. K. Mang, N. Kaneko, and M. Greven, Phys. Rev. Lett. **87**, 147003 (2001).
[44] N. P. Armitage, F. Ronning, D. H. Lu, C. Kim, A. Damascelli, K. M. Shen, D. L. Feng, H. Eisaki, Z.-X. Shen, P. K. Mang, N. Kaneko, M. Greven, Y. Onose, Y. Taguchi, and Y. Tokura, Phys. Rev. Lett. **88**, 257001 (2002).
[45] B. Stadlober, G. Krug, R. Nemetschek, R. Hackl, J. L. Cobb, and J. T. Markert, Phys. Rev. Lett. **74**, 4911 (1995).
[46] G. Blumberg, A. Koitzsch, A. Gozar, B. S. Dennis, C. A. Kendziora, P. Fournier, and R. L. Greene, Phys. Rev. Lett. **88**, 107002 (2002); F. Venturini, R. Hackl, and U. Michelucci, *ibid.* **90**, 149701 (2003).
[47] K. Tsutsui, T. Tohyama, and S. Maekawa, Phys. Rev. Lett. **83**, 3705 (1999).